Analysis and Prediction of Summer Rainfall over Southwestern Utah

John D. Horel[1] and James T. Powell[2]

[1]*University of Utah Department of Atmospheric Sciences*

Salt Lake City, UT

[2]*Radiometrics Corporation*

Submitted to: Weather and Forecasting

Corresponding Author: John D Horel, john.horel@utah.edu

ABSTRACT

While many studies have examined intense rainfall and flash flooding during the North American Monsoon (NAM) in Arizona, Nevada, and New Mexico, less attention has focused on the NAMS's extension into southwestern Utah. This study relates flash flood reports and Multi-Radar Multi-Sensor (MRMS) precipitation across southwestern Utah to atmospheric moisture content and instability analyses and forecasts from the High-Resolution Rapid Refresh (HRRR) model during the 2021-23 monsoon seasons.

MRMS quantitative precipitation estimates over southwestern Utah during summer depend largely on the areal coverage from the KICX WSR-88D radar near Cedar City, UT. Those estimates are generally consistent with the limited number of precipitation gauge reports in the region except at extended distances from the radar. A strong relationship is evident between days with widespread precipitation and afternoons with above average precipitable water (PWAT) and convective available potential energy (CAPE) estimated from HRRR analyses across the region.

Time-lagged ensembles of HRRR forecasts (initialization times from 03-06 UTC) that are 13-18 h prior to the afternoon period when convection is initiating (18-21 UTC) are useful for situational awareness of widespread precipitation events after adjusting for underprediction of afternoon CAPE. Improved skill is possible using random forest classification relying only on PWAT and CAPE to predict days experiencing excessive (upper quartile) precipitation. Such HRRR predictions may be useful for forecasters at the Salt Lake City National Weather Service Forecast Office to assist issuing flash flood potential statements for visitors to national parks and other recreational areas in the region.

SIGNIFICANCE STATEMENT

Summer flash floods in southwestern Utah are a risk to area residents and millions of visitors annually to the region's national parks, monuments, and recreational areas. The likelihood of flash floods within the region's catchments depends on intense afternoon and early evening convection initiated by lift and instability primarily due to terrain-flow interactions over elevated plateaus and mountains. Forecasts at lead times of 13-18 h of moisture and instability from the operational High Resolution Rapid Refresh model have potential to predict summer afternoons that are likely to have increased risks for higher rainfall amounts across southwestern Utah, although they are not expected to predict the likelihood of flash floods in any specific locale.

1. Introduction

The summer North American Monsoon (NAM) is responsible for frequent intense convection along the Mexican cordillera and over the mountain ranges of the Southwestern United States (Douglas et al. 1993; Dunn and Horel 1994a, b; Maddox et al. 1995; Adams and Comrie 1997; Yang et al. 2019; Boos and Pascale 2021). Many studies have looked at the conditions leading to extreme precipitation events associated with the NAM in this region and ways to predict their occurrence (Gutzler et al. 2009; Serra et al. 2016; Risanto et al. 2021). Not surprisingly, the fundamental building blocks for intense convection are necessary: lift, instability, and moisture (Doswell et al. 1996). Afternoon surface heating of elevated terrain provides the orographic lift that aids thunderstorm development (Maddox et al. 1979, Schumacher 2017). Mazon et al. (2016) classified extreme NAM weather events primarily in Arizona based on atmospheric instability, precipitable water vapor, and upper level conditions.

Smith et al. (2019) provide a detailed climatological evaluation of the seasonality and locations of thunderstorms in northern Arizona and southern Utah. Their study was motivated by flash floods in Hilldale, UT and within Zion National Park on 14 September 2015 that resulted in 20 fatalities, which account for nearly two-thirds of the total flash flood deaths during the past 25 NAM seasons in southwestern Utah. They note on the basis of lightning, radar, and streamflow records that the underlying terrain and synoptic/mesoscale setting modulate the occurrence and track of thunderstorms within the region. They also note that flash flood water volumes in the region's watersheds are unrelated to basin scale, as is often the case in other regions of the United States where flash flooding may result from widespread heavy precipitation. Rather, the flash flood response is tied to the spatial scale of thunderstorms (10-50 km^2) and their proximity to the small catchments upstream of slot canyons and channel narrows.

Figure 1 illustrates the seven-county region of southwestern Utah that is the focus for this study. This 64,000 km^2 region, larger than 10 U.S. states, encompasses low-lying deserts and scattered forests confined generally to the slopes and high plateaus of the western extent of the Colorado Plateau region. Prominent high elevation features of the region include from west to east the Pine Valley Mountains and Markagunt, Paunsaugunt, Kaiparowits, and Aquarius Plateaus. The Cedar City WSR-88D radar is sited at an elevation of 3230 m on the Markagunt Plateau (Fig.1). Although there are only ~200,000 permanent residents in the region, over 10 million visits are recorded annually to the national parks, monuments, and recreation areas within the region. Zion

National Park alone receives over 5 million visits while the other major destinations (Bryce, Capitol Reef, and Glen Canyon) receive between 1-3 million visitors annually.

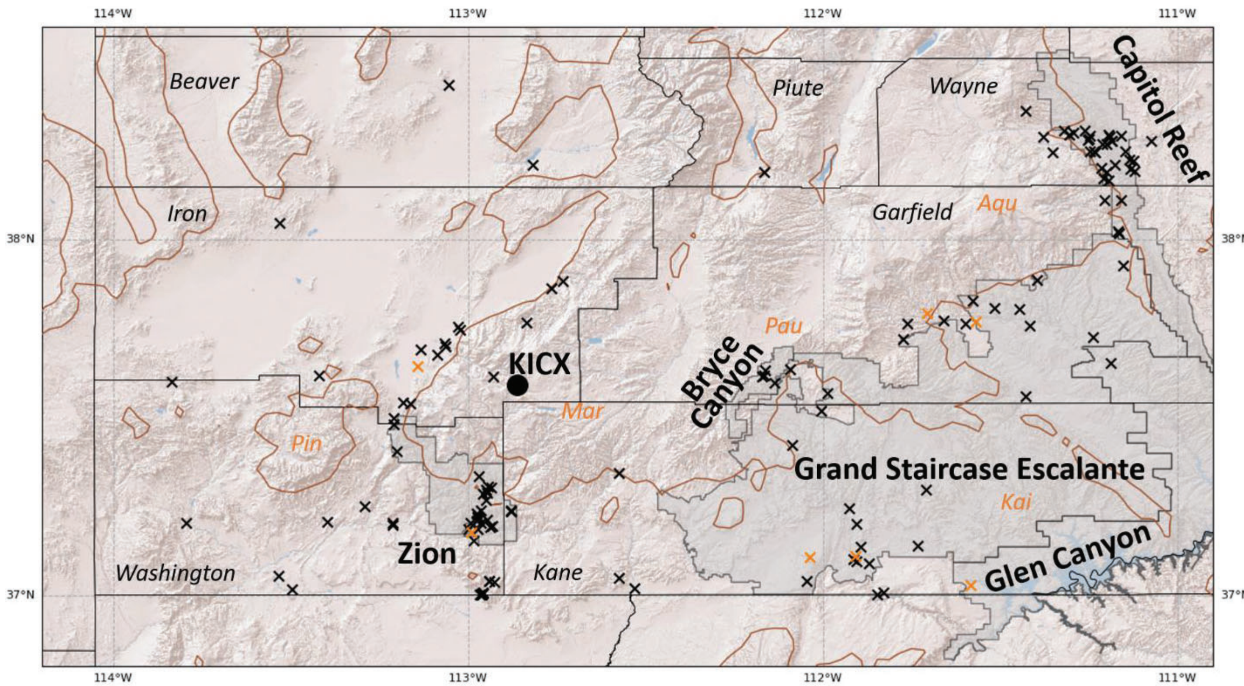

Fig. 1. Southwestern Utah with shaded terrain, brown 2000 m elevation contour, and black county outlines and labels. Light gray shading denotes national parks, monuments, and national recreation areas. Flash flood reports during the 2021-2023 summer seasons are indicated by cross symbols with locations of seven flash flood reports on 26 July 2021 in orange. The location of the Cedar City WSR-88D (KICX) is shown as well as general areas labeled in orange for the Pine Valley Mountains (Pin) and Markagaunt (Mar), Paunsaugunt (Pau), Kaiparowits (Kai), and Aquarius (Aqu) Plateaus.

Abrupt step-wise drops from the plateaus down to the desert floors are broken up by narrow riverine channels and slot canyons that contribute to the propensity for flash floods in the region. Quantifying the actual number of flash flood events in any region is difficult (Marjerson et al. 2016). The flash flood reports during the past three monsoon seasons (2021-2023) in southwestern Utah cluster near the small number of towns and cities located near canyon exits and in the elevation band of the Grey and White Cliffs (~1500-2500 m) within the parks, monuments, and recreation areas, hereafter referred to simply as Parks (Fig. 1). As summarized in Fig. 2, 745 flash floods in southwestern Utah have been reported to the National Center for Environmental Information (NCEI 2023) during the 1996-2023 period with the highest totals during 2013, 2021, and 2022. Of the 745 floods, 86% of them have been reported from May-September due to convective storms with 33 deaths and over $40 million dollars in property damage.

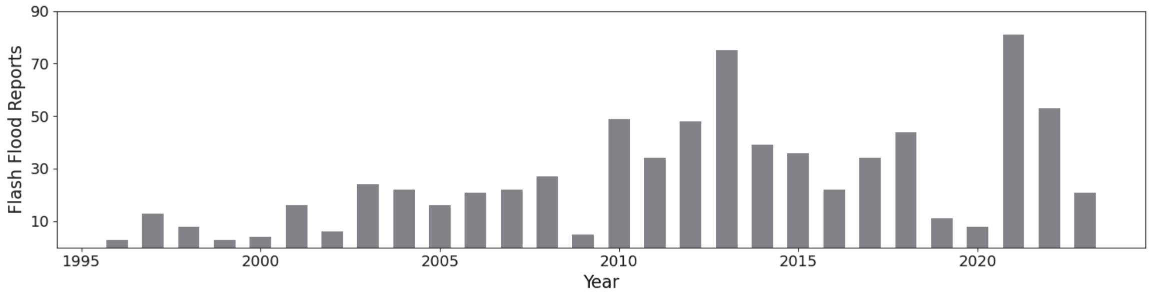

Fig. 2. Flash flood reports in the seven-county region of southwestern Utah during each year. (NCEI 2023).

Forecasting flash floods at short lead times (<6 h) often leads National Weather Service (NWS) offices to issue flash flood warnings (i.e., flash flood conditions occurring or imminent) that rely on careful evaluation by forecasters of model guidance, interpretation of satellite and radar imagery of convective environments, and situational awareness of flood-prone locales (Gourley et al. 2012; Yussouf et al. 2019, Martinaitis et al. 2023). The NWS Forecast Offices in Salt Lake City and Grand Junction issued for Utah the first and third highest numbers of flash flood warnings within the 1996-2023 period during 2021 and 2022, respectively (NCEI 2023).

Providing forecasts for the potential for organized convection and intense rainfall that might lead to flash floods within areas of complex terrain at lead times longer than 6 h requires greater reliance on numerical model output from operational convection allowing models, such as the High Resolution Rapid Refresh (HRRR; Sun et al. 2014; Blaylock and Horel 2020; Dowell et al. 2022; Grim et al. 2024). The NWS issues flood watches for such lead times. However, in order to avoid too many watches during the monsoon season, the Salt Lake City NWS Forecast Office (hereafter SLC WFO) issues flood watches typically on days when many basins are likely to be impacted. In addition, they issue forecasts of flash flood potential for the current and following day to eleven government entities responsible for public safety across Utah. Flash flood potential forecasts are provided in southwestern Utah for the regions highlighted in Fig. 1: Bryce National Park, Capitol Reef National Park, Glen Canyon National Recreation Area, Grand Staircase-Escalante National Monument, and Zion National Park.

This study focuses on the meteorological conditions in southwestern Utah during the 2021-2023 summer monsoon seasons associated with high intensity precipitation episodes that might lead to flash flooding. Of course, the occurrence of flash floods in this region and elsewhere depends on the complex interplay between terrain, soil and hydrologic factors (Smith et al. 2019, Hill and Schumacher 2021). We examine conditions between 15 June and 15 September when high risks exist in vulnerable locations for recreational injuries and fatalities, general public safety, and property damage. In addition, the availability of the Cedar City NWS radar within this region provides better estimation of convective activity and rainfall than is available for other parts of the state influenced by the NAM.

Large-scale conditions analyzed by the HRRR are summarized in this study for widespread and intense rainfall events during the three summers in southwestern Utah. Day-to-day variability is contrasted during the three summers for precipitation, flash flood reports, moisture availability, and instability. Conditions during the afternoon of 26 July 2021 are presented when rainfall in excess of 4 cm fell in Cedar City, UT and flash floods were recorded at six other locations within the region (Fig. 1).

Motivated by the lead time needed by Salt Lake City NWS forecasters to consider numerical guidance prior to issuing their first flash flood potential forecasts for the current day, we evaluate the utility of HRRR 3-h time-lagged ensemble (TLE) forecasts of precipitable water (PWAT) and maximum convective available potential energy (CAPE) issued 13-18 h prior to the afternoon period when convection is initiating across the region (18-21 UTC; 12-15 MDT). Our approach is to test whether forecasts of high PWAT and CAPE averaged over the entirety of southwestern Utah may identify days likely to experience unusually-high rainfall amounts across the region. We rely on hourly quantitative precipitation estimates (QPEs) from the Multi-Radar Multi-Sensor (MRMS) system (Martinaitis et al. 2021) to validate the HRRR model guidance. Of course, there has been no expectation from the outset of this study that HRRR forecasts at these lead times will provide an indication of the specific regions where intense rainfall may fall or flash floods may occur in specific catchments.

This research builds upon the study completed by Powell (2023) that examined the active summer monsoon seasons during 2021 and 2022. The results from that study have been expanded upon by examining conditions during the weaker 2023 monsoon season. Since prior studies and forecaster experience highlight that moisture availability and instability are dominant factors for intense NAM precipitation (Mazon et al. 2016, Smith et al. 2019; Yang et al 2019, Yu et al. 2023), we hypothesized that HRRR TLE ensemble forecasts of high PWAT and CAPE would be related to widespread rainfall in southwestern Utah. That hypothesis is evaluated using statistical approaches including bias correction and random forest classification (Brieman 2001, McGovern et al. 2017, Spieser et al. 2019, Chase et al. 2022). The successful operational implementation of random forest approaches to predict excessive rainfall events on a national scale has been demonstrated by Schumacher et al. (2021) and such approaches also are considered as part of the excessive rainfall outlooks of the Weather Prediction Center (Burke et al. 2023). In addition, staff at the SLC WFO tested random forest methods for flash flood predictions across southern Utah (D. van Cleave, 2023, personal communication). We divide the 2021 and 2022 summers into training and validation samples for random forest predictions followed by independent forecasts for summer 2023.

2. Data

a) Precipitation, Radar, and Lightning Observations

Although providing limited coverage across southwestern Utah, precipitation observations from 101 stations from the networks listed in Table 1 were available during all 3 summers. These networks were selected based on the sensor quality and likelihood of routine maintenance. For individual case studies, all available stations measuring rainfall were considered, which typically provided reports from over 50 additional sites within southwestern Utah. Precipitation observations were obtained using accumulated precipitation calculation services developed by Synoptic Data PBC.

Identifier	Description	No. Stations
RAWS	Interagency Remote Automatic Weather Stations	28
SNOTEL	Natural Resources Conservation Service	26
UCC	Utah Climate Center	13
SCAN	Soil Climate Analysis Network	10
ASOS	National Weather Service/Federal Aviation Administration	9
HADS	Hydrometeteorological Automated Data System	7
PACIFICORP	PacifiCorp Utility	6
CRN	Climate Reference Network	2

Table 1. Number of stations in southwestern Utah from selected networks reporting precipitation during all three summers.

Deep convection within southwestern Utah is generally detected by the Cedar City WSR-88D Doppler RADAR (KICX). This radar is located 3230 m above sea level near the southwestern edge of the Markagunt plateau (Fig. 1). Due to its high elevation, 0.2 degree elevation scans are available to help identify conditions over the surrounding desert regions at elevations typically between 1000-2000 m.

Widespread coverage of vigorous convection containing lightning is made possible from the ground-based National Lightning Detection Network (NLDN; Murphy et al. 2021). The Flash Energy Density (FED) product provided by the MRMS system that is based upon the NLDN is used in this study. FED is an estimate of the number of cloud-to-ground flashes per km^2 during each 30-minute period.

b) Radar Multi-Sensor Quantitative Precipitation Estimates

The MRMS is an operational system of the National Centers for Environmental Prediction for estimating precipitation from radar, rain gauge, satellite, lightning, and numerical weather model data (Zhang et al. 2016; El Saadani et al. 2018; Sharif et al. 2020, Martinaitis et al. 2021). The MRMS Quantitative Precipitation Estimate (QPE) Pass II product for each hour and for each km^2 along with FED and other diagnostic fields were accessed from Iowa State University's Iowa Environmental Mesonet archive (Iowa State University 2023).

Radar precipitation estimates are the primary input for MRMS QPE in southwestern Utah. MRMS processing involves quality control applied to radar data (e.g., accounting for beam blockage and non-precipitation echoes) and provides a radar quality index for each location (Martinaitis et al. 2021). If an area has adequate radar quality, radar estimates may be adjusted using weighted corrections based on precipitation gauge data to then yield the final QPE. Gauges from many of the networks listed in Table 1 are not incorporated into the MRMS QPE and hence are helpful to evaluate the accuracy of the QPE estimates. If the radar quality is poor during convective situations, precipitation estimates may be adjusted based on gridded estimates of precipitation from the HRRR model.

c) High-Resolution Rapid Refresh Model

The HRRR is a convection allowing, short-range forecast model with 3km horizontal grid spacing run operationally every hour by the National Centers for Environmental Prediction for the

CONUS region (Dowell et al. 2022, Grim et al. 2024). Forecasts at lead times out to 18 h are available every hour with lead times extended out to 48 h at 00, 06, 12, and 18 UTC. The HRRR benefits from advanced data assimilation techniques incorporating standard data observations (rawinsonde, aircraft, GPS precipitable water, etc.) and also includes 3-D radar reflectivity data from the MRMS and lightning data from the NLDN (Hu et al. 2017; James and Benjamin 2017; Dowell et al. 2022). Access to the high-resolution forecast model output in grib2 format is currently available through Amazon Web Services and Google's Cloud Platform (Dowell et al. 2022). This study relies on HRRR version 4 that was deployed on 2 Dec 2020. Model analysis (F00) and forecast (F01-F18) fields are retrieved in Zarr format from Amazon Web Services (Gowan et al. 2022). Supported by Amazon's Sustainability Data Initiative, the Zarr files are created in order to split the CONUS into 96 compressed chunks, allowing more efficient downloading for smaller domains (Gowan et al. 2022).

HRRR model F00 analyses and F12-F18 forecasts of deep moisture (PWAT) and instability (surface-based CAPE) are relied upon extensively in this study as a means to assess conditions favorable for widespread convection across southwestern Utah. Mazon et al. (2016), Yang et al. (2019), and Yu et al. (2023) used similar metrics to study the NAM in Arizona and Nevada. Surface-based CAPE was found to be an adequate metric for estimating the potential for convective instability over elevated terrain due to the limited convective inhibition likely in these locations during summer afternoons.

HRRR QPE at 06-18 h lead times was compared to MRMS QPE and NLDN FED as a means to assess the extent to which those forecasts might be useful for situational awareness for the likelihood of widespread precipitation across southwestern Utah. However, HRRR QPE forecasts substantially underestimated observed and analyzed precipitation in southwestern Utah. Hence, we do not rely on HRRR QPE forecasts in this study.

3. Results

a) 26 July 2021

Substantial property damage due to flash flooding occurred on 26 July 2021 near Cedar City, UT. Seven flash flood reports were made on this day (Fig. 1). PWAT and CAPE analyzed by the HRRR during this afternoon from 18 UTC 26 July to 00 UTC 27 July (12-18 MDT) are shown in Fig. 3. The northerly moisture transport into Arizona, Nevada, and Utah was extensive (Fig. 3a) with local CAPE values in excess of 2000 J kg^{-1} across southwestern Utah (Fig. 3b). The areal- and daily- averaged PWAT in this case was 2.7 cm and areal-averaged maximum CAPE was 900 J kg^{-1}.

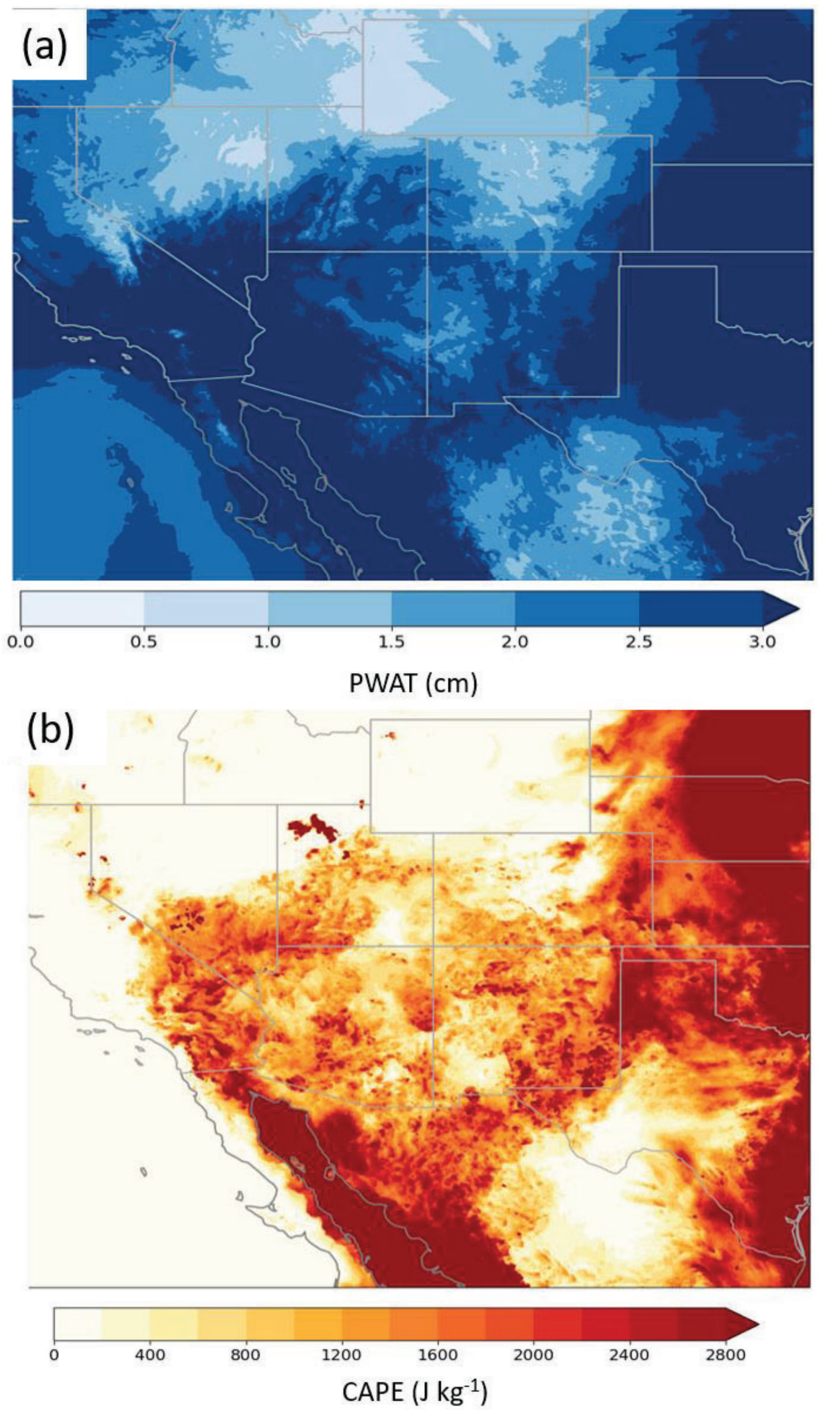

Fig. 3. (a) Mean hourly HRRR PWAT (cm) during the period 12 – 18 MDT 26 July 2021. (b) Maximum hourly HRRR CAPE (J kg^{-1}) during the same period.

The prevailing flow during this afternoon was deep southeasterly winds from 700 to 250 hPa (not shown). Animations of GOES-West satellite imagery and KICX composite radar reflectivity during this afternoon confirmed the prevailing southeast to northwest progression of thunderstorm cells during the afternoon as shown by the composite radar reflectivity during the afternoon (Fig. 4a). Figure 4b shows the average hourly FED during 12-18 MDT with many areas exhibiting extensive lightning across southwestern Utah including frequent lightning near Cedar City and the other locations reporting flash flooding that afternoon.

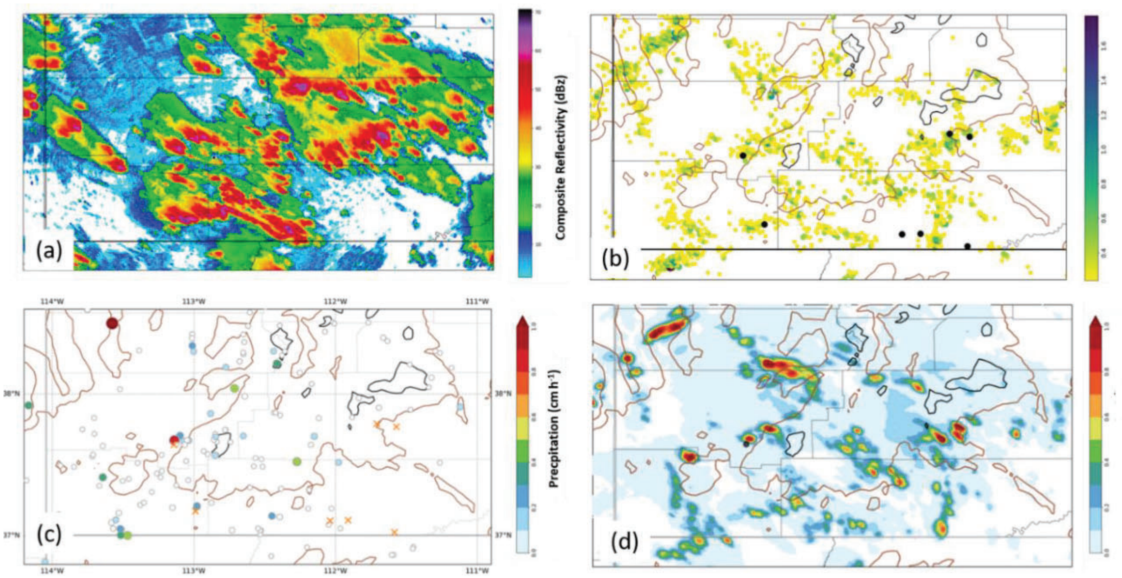

Fig. 4. (a) Maximum composite reflectivity (dBz) from the KICX radar during 13 – 14 MDT 26 July 2021. (b) Average NLDN FED (strikes km^{-2} h^{-1}) during the period 12 – 18 MDT 26 July 2021. Black dots show the locations of flash flood reports that day. Heavy solid lines denote terrain elevation at 2000m (brown) and 3000m (black). (c) Average hourly precipitation (cm h^{-1}) during the period 12 – 18 MDT 26 July 2021. The locations of the flash flood reports are indicated by orange x's. (d) As in (c) except from MRMS analyses.

Average hourly precipitation rates during the afternoon from 136 stations and MRMS QPE analyses during the afternoon are shown in Figs. 4c and 4d, respectively. While modest amounts of rainfall were observed across many areas of southwestern Utah during this afternoon, excessive amounts were highly localized, most notably reports of over 7 and 4 cm during the 6 h period at the Utah Climate Center stations located in the Wah Wah Range and Cedar City, respectively (denoted by the two red circles in Fig. 4c). While no reports of flooding are available from the remote Wah Wah site near the northwestern edge of the domain, reports of flooding across the

Interstate southwest of Cedar City were associated with a strong cell (maximum composite reflectivity > ~65 dBz) from 14-15 MDT (not shown). Much of this precipitation was channeled directly into residential and commercial areas of Cedar City, a city with 37,000 residents. The MRMS precipitation analyses for this afternoon capture many of the cells associated with the flash flood reports (Fig. 4d) as well as near Wah Wah, even though beam blockage affected radar returns in that area. The latter was likely due to the use of lightning data by the MRMS since that Utah Climate Center station was not assimilated into the MRMS.

Seasonal Summaries

Figure 5a highlights the average daily precipitation (mm) during the 2021-2023 summer seasons (15 June to 15 September) from 675 stations from the networks listed in Table 1 that are available in Utah and adjacent areas. While very helpful, these observations are clearly insufficient to capture the strong gradients in rainfall that take place across the region from desert lowlands to Utah's high elevation mountain ranges. High daily averages (2.5-3 mm) during these three summers among the 101 stations within southwestern Utah are found on the Markagunt Plateau near the KICX radar.

The spatial variability in the three-summer average of MRMS daily rainfall is shown in Fig. 5b. Mazon et al. (2016) highlighted the climatologically lower rainfall totals in the NAM's extension into southern Utah compared to those in northern Arizona. As expected, all of the mountain ranges and plateaus of southwestern Utah exhibit higher MRMS QPE than their surrounding deserts (e.g., from west to east the Pine Valley Mountains and Markagunt, Paunsaugunt, Kairparowits, and Aquarius Plateaus). The 50-75th MRMS QPE percentiles within 25 km of KICX on the Markagunt Plateau lie between 2.5-3 mm day^{-1}, which is consistent with the observations in that region. However, some of the isolated ranges in central and eastern Utah (e.g., Henry and Abajo Mountains) far from KICX and the Grand Junction, WY radar (KGJX) have higher gauge totals than MRMS QPE. Based on prior research (e.g., Herman and Schumacher 2018), feedback from NWS forecasters and comparing MRMS QPE to station observations, NLDN FED, and HRRR short range forecasts during the 2021 and 2022 summer seasons, Powell (2023) concluded that the lack of radar coverage for such mountain ranges likely impacts the MRMS QPE estimates in the peripheries of the southwestern Utah domain.

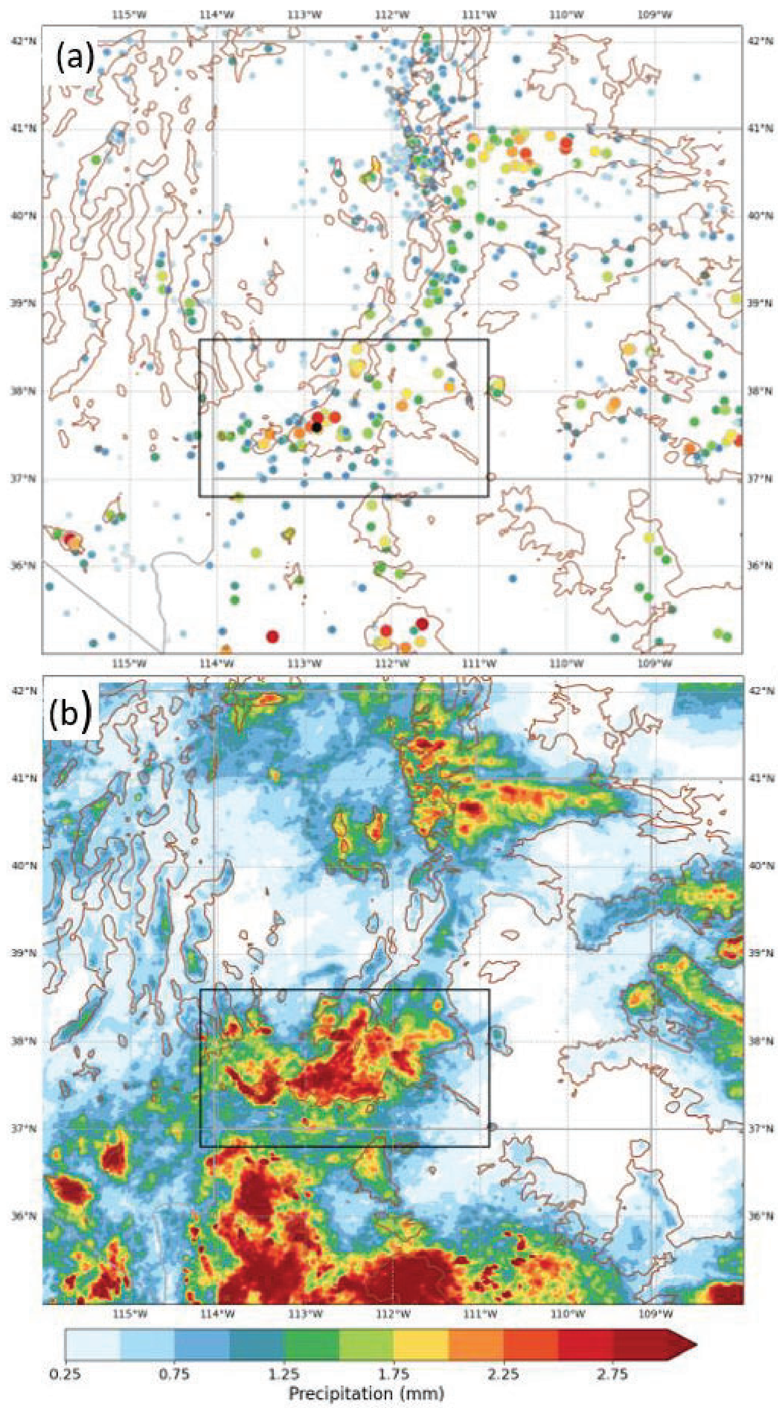

\

Fig. 5. (a) Observed average daily precipitation (mm) shaded according to the scale at the bottom for stations in the networks listed in Table 1 during the 2021-2023 summer seasons from 15 June to 15 September. KICX WSR-88D radar location denoted by the black circle and the brown contours denote 2000 m elevation. The rectangle encloses the southwest Utah region. (b) As in (a) except for MRMS analyzed values of average daily precipitation.

As documented previously by Smith et al. (2019), deep convection in the region initiates around solar noon over the high plateaus and mountains and, depending on the prevailing flow, persists there or propagates away later during the afternoon and evening. Figure 6a illustrates that initial development between 12-15 MDT (18-21 UTC). For the region as a whole, the highest rainfall totals occur between 15-18 MDT (Fig. 6b) and then diminish during the evening (Fig. 6c). Maxima across the region of average rainfall totals during the other 3 h periods are below 0.4 mm day^{-1} (not shown).

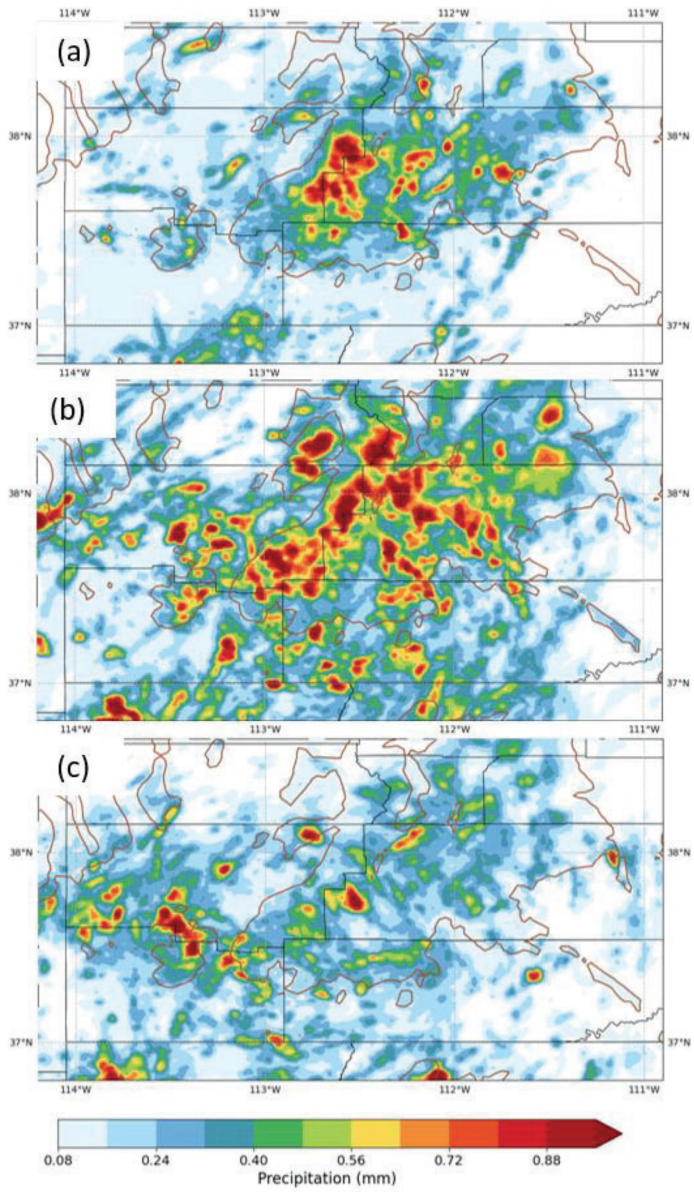

Fig. 6**.** MRMS 3-h QPE totals (mm) averaged over the three summers for: (a) 12-15 MDT; (b) 15-18 MDT; (c) 18-21 MDT. Brown contours denote 2000 m elevation.

The accumulation of flash flood reports during the three summer seasons is presented in Fig. 7a. As mentioned earlier, the number of flash flood reports in the region depends on observers being present as well as favorable meteorological conditions leading to intense convection and hydrologic factors near specific vulnerable locales. The total number of flash flood reports was highest during 2021 and fewest in 2023 (see also Fig. 2). Intense convection leading to flash floods began in earnest during mid-July 2021 while the number of flash floods reported increased sharply during the mid-August 2022 monsoon period. While flash floods were reported on similar numbers of days during 2021 and 2022, they were reported on only 10 days during summer 2023.

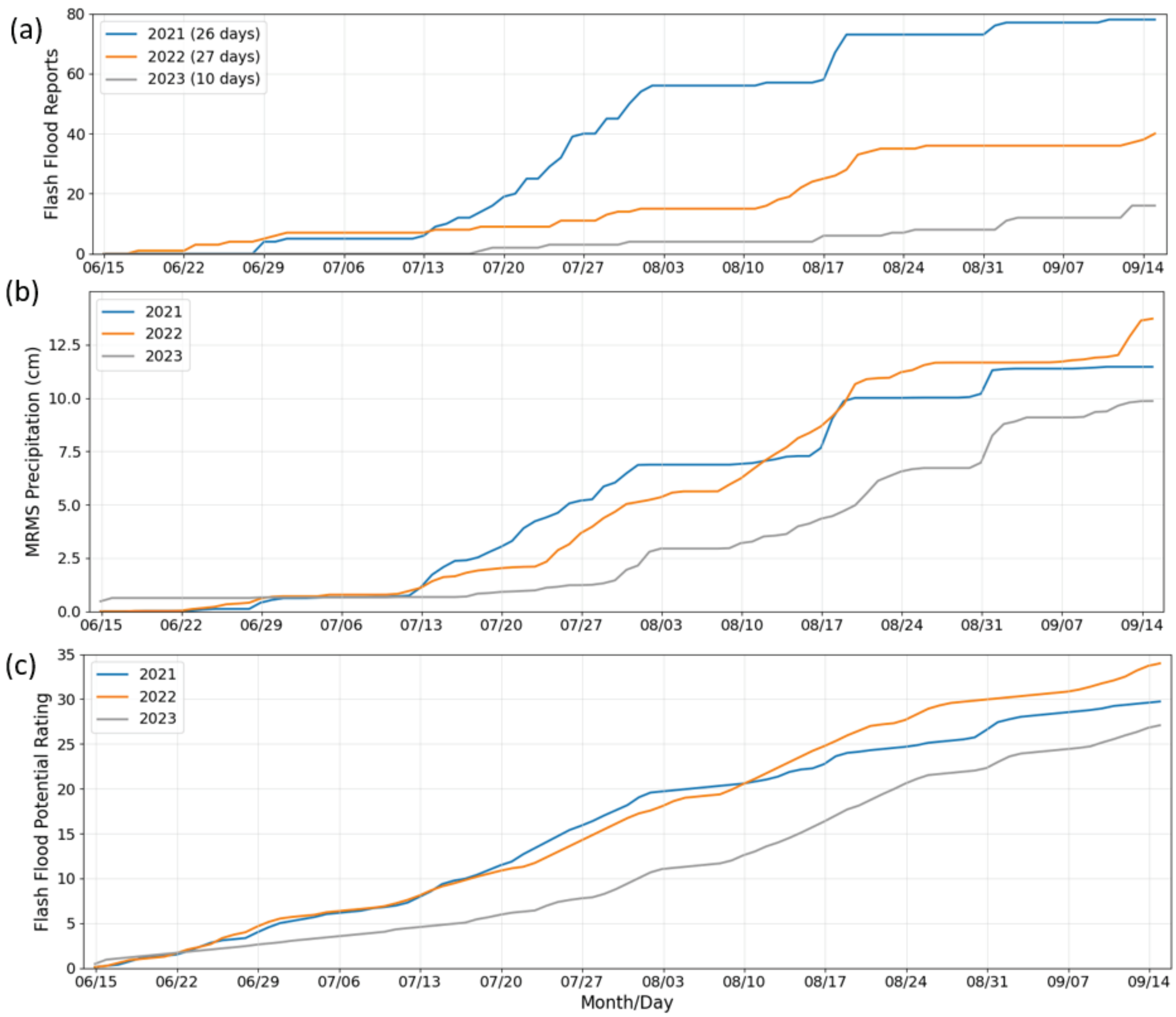

Fig. 7. a) Accumulated flash flood reports during each summer season. b) Accumulated daily precipitation (cm) averaged over southwestern Utah during each summer. c) Accumulated mean daily Flash Flood Potential Rating forecasts issued by the SLC WFO for southwestern Utah.

The accumulation during each season of daily MRMS QPE averaged over the entire southwestern Utah domain is shown in Fig. 7b. Although only half as many flash floods were observed during summer 2022 compared to 2021, the accumulated precipitation across the domain was higher during that summer. In addition, even though the 2023 NAM had a delayed start until mid-July, the accumulated seasonal rainfall was comparable to that observed in 2021. Less intense precipitation likely fell in regularly-monitored flood prone regions during summer 2023 compared to that during the other two years.

As mentioned earlier, Salt Lake City NWS forecasters have extensive experience issuing watches and warnings for flash flood conditions across southwestern Utah on the basis of many data and numerical model resources. Based on their experience and recommendations from constituents, the flash flood potential ranking (FFPR) was developed and is now issued by the SLC WFO to benefit government agencies responsible for public safety in the Parks. FFPR values are first issued for the current and next day typically in the early morning (8-10 UTC; 2-4 MDT) and then updated as necessary throughout the day. Figure 7c summarizes the issuance of the initial FFPRs for the five Parks indicated in Fig. 1. While Park staff prefer that the FFPR be defined by text descriptors, Salt Lake City forecasters have assigned loose probabilities of flash flood occurrences to them as follows: Not Expected (12.5%), Possible (37.5%), Probable (62.5%), and Expected (87.5%). The daily values accumulated in Fig. 7c are the average of those probability values (0-1) computed from the five Park forecast sample.

The FFPR trends during each summer follow the trends in areal-averaged rainfall (Fig. 7b) rather than flash flood reports (Fig. 7a), e.g., the highest risk overall for flash flooding was predicted to be during summer 2022. In addition, specific monsoonal periods with larger average rainfall also were periods when FFPR forecasts were higher (e.g., late July and early September 2023).

b) Forecasting Widespread Rainfall

As mentioned in the introduction, an objective of the study by Powell (2023) and this work was to test whether HRRR model guidance at lead times between 13-18 h would be useful for predicting afternoons most likely to have widespread rainfall across southwestern Utah. Our TLE approach shown schematically in Fig. 8 builds on the capability to use hourly updating HRRR forecasts and prior work that has relied on HRRR TLEs (e.g., Thompson et al. 2017, Xu et al. 2019, Gowan et al. 2022). The sample of initialization times we use (3-5 UTC) are motivated by the lead time needed by Salt Lake City NWS forecasters to consider numerical guidance prior to issuing overnight their first FFPR forecasts for that afternoon. As shown in Fig. 8, a sample of 12 PWAT forecasts and maximum CAPE are available 13-18 h prior to the afternoon period when convection is initiating across the region (18-21 UTC; 12-15 MDT). Hence, to gain additional lead time given that HRRR forecasts are available each hour only at lead times up to 18 h, we focus on the conditions when convection is starting (Fig 6a), rather than when the convection and rainfall reaches its peak (Fig. 6b). We test whether the ensemble average forecasts of high PWAT and CAPE averaged over the entirety of southwestern Utah may identify days likely to experience unusually-high rainfall amounts across the region.

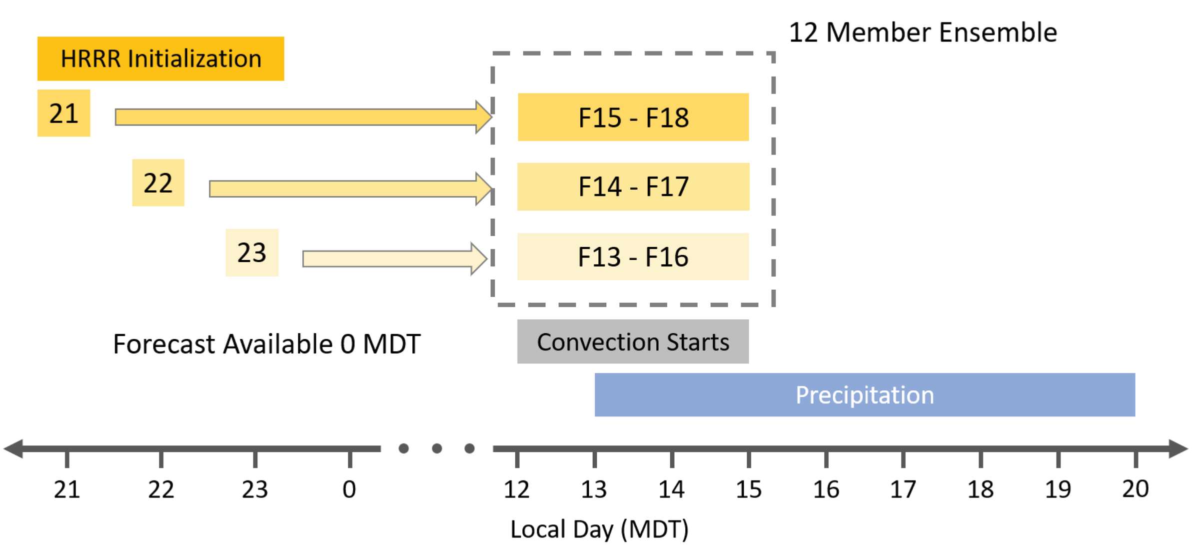

Fig. 8. Twelve-member Time-Lagged Ensemble forecasts for the early-afternoon period during which convection typically starts in southwestern Utah are generated from HRRR forecasts initialized from 21-23 UTC the previous evening.

The seasonal trends in ensemble mean PWAT analyses averaged over southwestern Utah during early afternoon exhibit relatively monotonic increases of 0.75-1.0 cm day^{-1} with higher totals during summer 2022 than the other two summers (Fig. 9a). The average PWAT of the TLE forecasts valid during those same afternoon periods (dashed lines) are slightly lower than analyzed during all three summers, which reflects a very small dry bias of HRRR forecasts. Similar to the seasonal evolutions of rainfall (Fig. 7b), the seasonal accumulation of maximum CAPE based on early afternoon HRRR analyses exhibit periods when the NAM is more active in this region than other periods (Fig. 9b). Higher CAPE is also evident during summer 2022 than that during the other two summers. It should be noted that the analyzed CAPE values shown in this study over southwestern Utah may underestimate actual conditions. Prior work with earlier versions of the HRRR found the analyses had a stable bias compared to estimates from rawinsondes (Evans et al. 2018). Of greater importance is the clear bias of the CAPE forecasts to be more stable than analyzed (Evans et al. 2018; MacDonald and Nowotarski 2023). This deficiency also likely contributes to dry biases of HRRR model precipitation forecasts (Dougherty et al. 2021, Powell 2023).

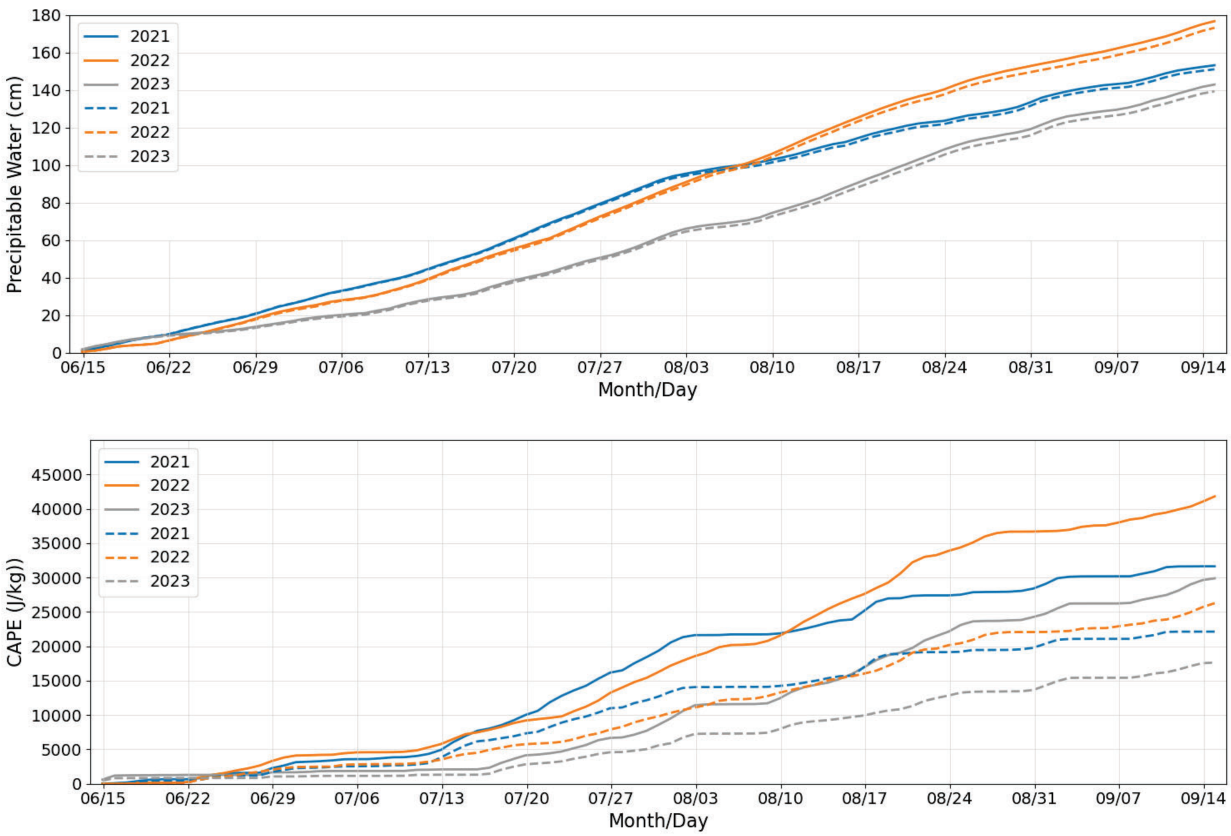

Fig. 9. a) HRRR PWAT (cm) analyses during 18 – 21 UTC (12 – 15 MDT) averaged over southwestern Utah and accumulated during each summer season (solid lines). HRRR TLE PWAT forecasts valid at the same time (dashed lines). b) As in (a) except for maximum hourly CAPE (J kg^{-1}).

Following the approach used by Mazon et al. (2016), Yang et al. (2019), and Yu et al. (2023), we relate regional PWAT and CAPE to daily mean QPE in Fig. 10 during all three summers. The large-scale CAPE values in Fig. 10a are domain averages of the maximum CAPE at every grid point during the 12-15 MDT period while the PWAT values are domain averaged PWAT during that time period. The size and color of each dot denotes the accumulated precipitation for that entire day, which predominantly falls between 12-21 MDT (Fig. 6).

As shown in Fig. 10a, MRMS QPE amounts tend to be low if either PWAT averaged over southwestern Utah is less than the three-year mean in PWAT (1.7 cm) or maximum CAPE is less than its three-year mean (390 J kg^{-1}), i.e., nearly all the high rainfall amounts are located in the upper right quadrant of Fig. 10a. Cross symbols in Figure 10a denote the 63 days when at least one NCEI flash flood report was recorded. Nearly all of those days lie as well in the upper quadrant of Fig. 10a (above normal PWAT and CAPE). Smith et al (2019) also found that lightning activity increased in the region when PWAT was greater than 1.5 cm and grew substantively after 2.0 cm. Hence, above normal CAPE and PWAT is a reasonable estimate for days likely to experience higher rainfall totals across the region and, to some extent, the number of days with flash flood reports.

Figure 10b relates the daily accumulated MRMS QPE to the ensemble mean forecasts of CAPE and PWAT. Comparing Figs. 10a and 10b, the downward shift in the days with high rainfall amounts and flash flood reports results from the large stable bias of HRRR CAPE forecasts evident as well in Fig. 9b without any substantive PWAT bias (Fig. 9a). Table 2 also illustrates the HRRR CAPE forecast bias. The counts of days and average rainfall along the diagonals summarize the cases when HRRR forecast conditions match those analyzed. HRRR CAPE forecasts underestimated analyzed CAPE on 37 days. Rainfall totals for the region on those days were often high.

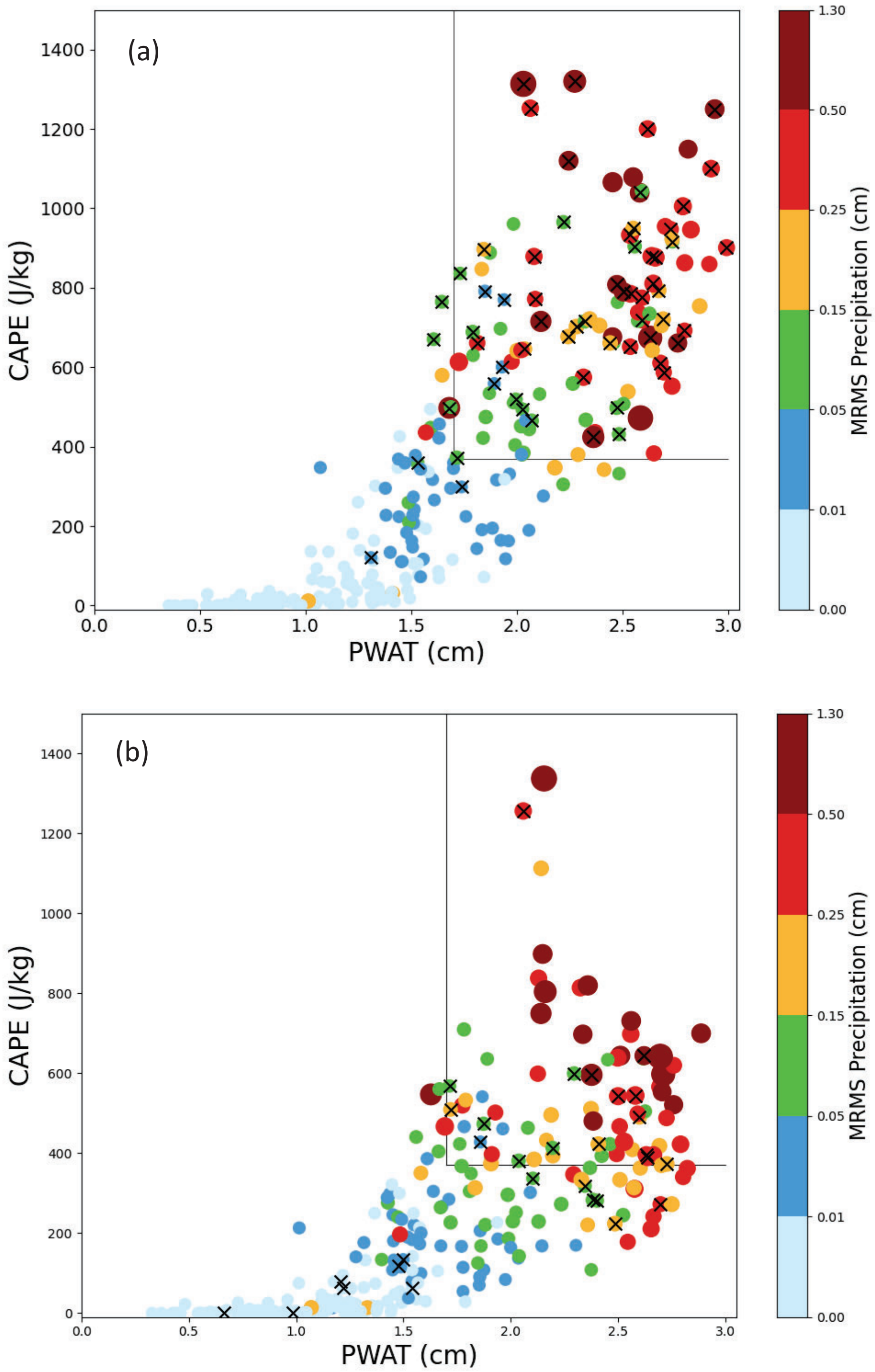

Fig. 10. (a) HRRR analyses of maximum PWAT (cm) vs. CAPE (J kg^{-1}) during 18-21 UTC (12-15 MDT) each day of the three summers averaged over southwestern Utah. The color and size of each circle denotes daily MRMS precipitation (cm). Cross symbols denote days with at least one flash flood report. The solid lines highlight the mean PWAT and CAPE. (b) As in (a) except for HRRR TLE ensemble mean forecasts of PWAT vs CAPE initialized between 3-5 UTC and valid at 18-21 UTC.

	PWAT-B; CAPE-B		PWAT-B; CAPE-A		PWAT-A; CAPE-B		PWAT-A; CAPE-A	
	Days	PPT	Days	PPT	Days	PPT	Days	PPT
PWAT-B CAPE-B	**136**	**0**	0	___	2	0.03	0	___
PWAT-B CAPE-A	8	0.09	**5**	**0.26**	0	___	0	___
PWAT-A CAPE B	2	0.02	0	___	**16**	**0.04**	1	0.23
PWAT-A CAPE-A	0	___	1	0.47	*37*	*0.17*	**71**	**0.34**

Table 2. Days and average daily precipitation (PPT, cm) for HRRR TLE forecasts (columns) relative to HRRR analyses (rows) during all three summers. Forecasts and analyses are subdivided whether Precipitable Water (PWAT) and Convective Available Potential Energy (CAPE) are Below (B) or Above (A) 3 season averages across southwestern Utah. Bold face denotes categorical Hits while italics highlight frequent underpredictions of CAPE.

Accounting for the large CAPE bias is a possible way to utilize HRRR predictions to identify those afternoons that might have enhanced convection. Compensating for both the PWAT and CAPE biases evident during the 2021 and 2022 summers (-0.03 cm and -135 J kg^{-1}), predictions for conditions during summer 2023 are shown in Table 3. The number of underestimates of above normal CAPE days drops from 34% (37 of 108) to 19% (6 of 31).

The predictions in Table 3 address identifying those afternoons during summer 2023 with above normal CAPE and PWAT that often are associated with higher rainfall amounts across southwestern Utah. An alternative approach is to identify ways to predict those days when daily MRMS rainfall amounts are unusually high (≥ 0.14 cm), approximately the top 25% of those observed during the 2023 summer. Figure 11a shows the analyzed MRMS rainfall amounts during each day of that summer. Several distinct heavier rainfall periods are evident: 15 – 16 June; 30 July – 3 Aug; 10 – 24 Aug; 31 Aug – 4 Sep; and 10 – 13 Sep. Figures 11b and 11c show the HRRR analyzed and TLE forecasted values for afternoon PWAT and CAPE, respectively. The general relationships evident in earlier figures are encapsulated here: TLE PWAT forecasts are nearly identical to those analyzed; TLE CAPE forecasts underestimate CAPE analyses; and periods when PWAT and CAPE are both high often have higher rainfall totals.

	PWAT-B; CAPE-B		**PWAT-B; CAPE-A**		**PWATA; CAPE B-**		**PWAT-A; CAPE-A**	
	Days	PPT	Days	PPT	Days	PPT	Days	PPT
PWAT-B CAPE-B	**52**	**0**	0	___	2	0.03	0	___
PWAT-B CAPE-A	2	0.14	**2**	**0.31**	0	___	0	___
PWAT-A CAPE-B	2	0.02	0	___	**4**	**0.10**	1	0.13
PWAT-A CAPE-A	0	___	1	0.15	*6*	*0.16*	**25**	**0.27**

Table 3. As in Table 2 except for the 2023 season only and after correcting for the small PWAT and large negative CAPE biases evident during the 2021 and 2022 seasons.

A predictive scheme patterned loosely on the FFPR is to classify days into three categories based on TLE prior-summer bias-corrected forecasts of PWAT and CAPE: (1) If they are both below normal, then having rainfall in the upper 25th percentile is “Not Expected”; (2) if only one parameter is above normal, then having high rainfall is “Possible”; (3) if both are above normal, then high rainfall is “Probable”. Table 4 summarizes the results of such a prediction scheme for the 2023 summer. Treating a Probable forecast as a Hit and using standard forecast metrics (Wilks 2011, Chase et al. 2022), this approach would yield the following scores: 63% Probability of Detection (POD); 58% Success Ratio (SR); and 43% Critical Success Index (CSI). Hits and False Alarms are indicated in Fig. 11a by the blue and orange triangles, respectively. Misses are days when the MRMS rainfall is above the solid line (~75th percentile) and there are no triangle symbols.

	Not Expected	**Possible**	**Probable**
MRMS< 0.14 cm	52	6	11
MRMS≥ 0.14 cm	2	7	15

Table 4. Bias-corrected HRRR PWAT and CAPE predictions of daily areal-mean MRMS precipitation exceeding ≥ 0.14 cm (~75th percentile) during the 2023 season relative to MRMS daily areal-mean precipitation.

The large number of False Alarms and Misses using this bias correction approach and the numerous machine learning studies recently examining way to predict extreme rainfall event (e.g., Hill and Schumacher 2021) led us to consider such approaches. However, rather than using a large number of predictor variables as is often used, we limited for clarity the predictors simply to PWAT and CAPE TLE mean forecast values. The arbitrary decision to target or label in terms of the relatively rare high rainfall days (MRMS $\geq$ 0.14 cm) lends itself to binary classification as opposed to predicting precipitation amount each day. The supervised random forest classification method is well suited for this application (Brieman 2001, Spieser et al. 2019, Chase et al. 2022). We subdivided randomly the days during the 2021 and 2022 summers into training and validation data sets (67% and 33% of the samples, respectively) leaving the entire 2023 summer as the test data set. The sklearn default threshold of 0.50 is used to discriminate between high and non-high rainfall days. Optimal hyperparameters were found to vary depending on the relative sizes of training and validation data sets, but the results applied to the 2023 test data set were invariant to these differences in maximum depth and number of estimators. The accuracy score was 0.93 with the relative feature importance of the two predictors being 53% and 47% for TLE PWAT and CAPE, respectively. It should be reiterated that this approach does not depend on bias correction- the predicted CAPE values are those underestimating what actually happened.

The results of the random forest classification are shown in Table 5 and Fig. 11a. The score metrics improve over the bias correction approach as follows: 83% POD; 77% SR; and 67% CSI. For the purposes of this study, it is unnecessary to attempt to maximize these scores from these relatively robust values. However, the selection of the 0.14 threshold was arbitrary and it is apparent in Fig. 11a that 4 of the 6 False Alarms resulted from rainfall amounts slightly below that level. In addition, two of the four misses resulted from a mid-latitude trough crossing the state during 15 – 16 June for which the PWAT is lower than typically found later during the monsoon season in this region.

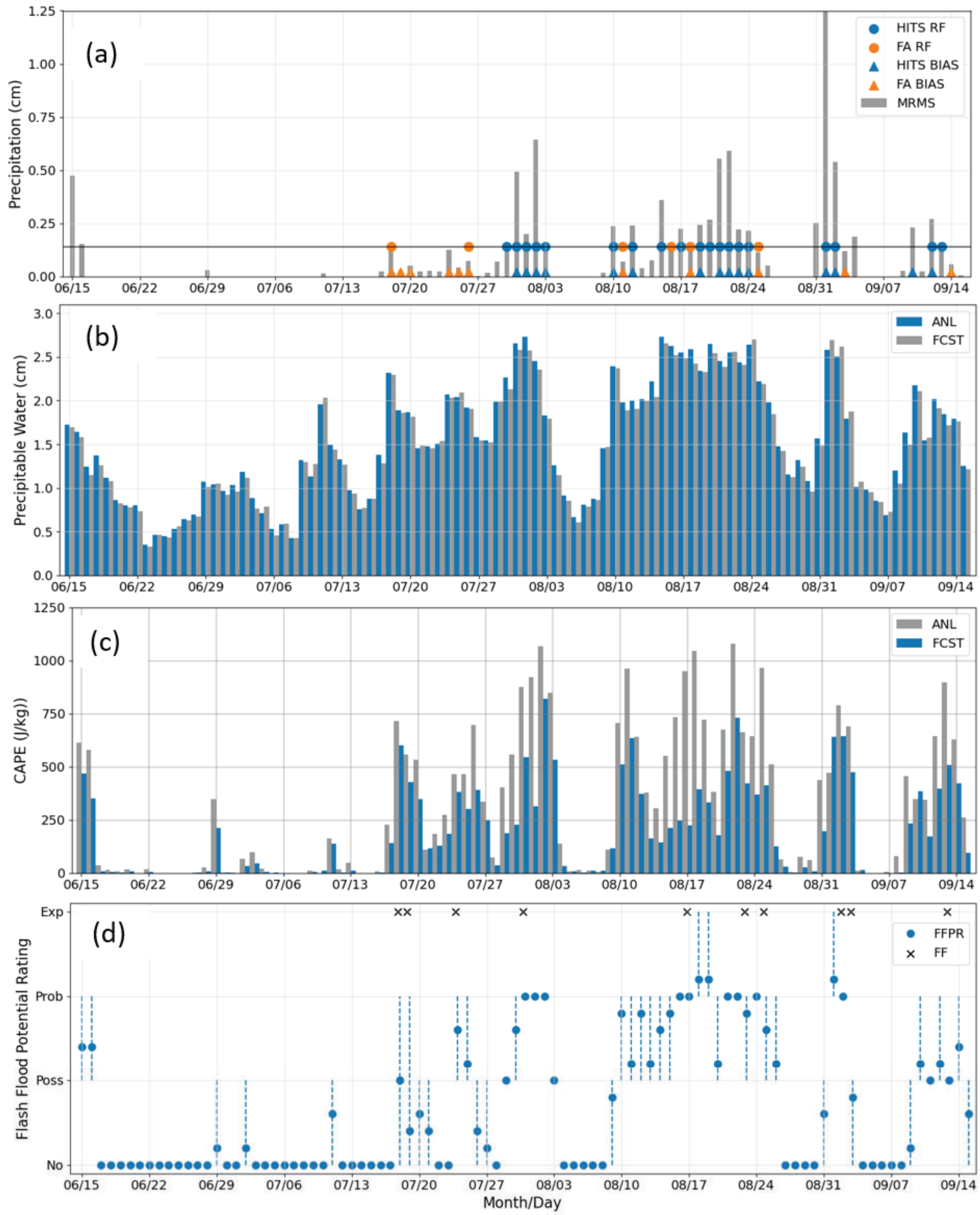

Fig. 11. (a) Daily MRMS rainfall (cm, bars) averaged over southwestern Utah during summer 2023. Symbols denote TLE forecast hits (blue) and false alarms (orange) for random forest (circles) and bias corrected (triangles) methods to predict rainfall exceeds the ~75th percentile (solid line). (b) PWAT (cm) from HRRR analyses (blue) and TLE forecasts (gray) for the 18-21 UTC period. (c) As in (b) except for

maximum CAPE (J kg^{-1}). (d) Mean (circles) and spread (dashed lines) of FFPR forecasts issued by the Salt Lake City NWSFO for the 5 Parks in southwestern Utah. Categorical forecasts made for each Park are: Not expected (No); Possible (Poss); Probable (Prob); Expected (Exp). Days with flash floods reported denoted by crosses.

While the purposes for the SLC WFO FFPR metric are highly focused on the specific needs of the Park staff to alert visitors to flash flood likelihood, it is instructive to compare the FFPR forecasts during the 2023 summer in Fig. 11d to the areal averages of MRMS QPE and HRRR analyses and TLE forecasts shown in the other panels of Fig. 11. It should come as no surprise that Probable or Expected predictions of flash floods at multiple Parks are made when PWAT and CAPE tend to be high. The onset of the monsoon season on 18-19 July illustrates cases when intense localized thunderstorms led to flash floods in Capitol Reef National Park yet had less-intense rainfall across the entire region. These two days had the largest FFPR forecast spread across the five Parks with the forecasters anticipating flash conditions to be Probable at Capitol Reef on both days and Possible or Not Expected at the other four Parks. Note that the bias-corrected and random forest forecasts overestimated the areal coverage of rainfall to be expected on those days.

	Pred < 0.14 cm	**Pred ≥ 0.14 cm**
MRMS< 0.14 cm	63	6
MRMS≥ 0.14 cm	4	20

Table 5. As in Table 4 except for random forest classification predictions based on TLE PWAT and CAPE.

4. Summary

The NAM brings intense rainfall frequently during summer to Mexico and the southwestern United States. Occasionally, flash floods in vulnerable locales within southwestern Utah lead to injuries, fatalities and damage in population centers as well as heavily visited Parks. The analysis of the 2021-2023 seasons was focused on identifying the basic conditions conducive to intense rainfall over southwestern Utah that may lead to flash floods in the preferred areas that experience them. Rapid rainfall rates over the sparsely visited elevated plateaus or desert floors of the region will have less impact than those in the vicinity of the "risers" of the region's "stairs" where streamflow is constricted, previous wildfires have affected soil permeability, or where visitors congregate for recreational activities.

The 2021 and 2022 summers in southwestern Utah were two of the most active monsoon seasons on record leading to high numbers of flash flood reports. The 2023 monsoon season was delayed and rainfall amounts across the region were somewhat lower than during the other two summers. However, the reduced number of flash flood reports during that season likely resulted more from the relative randomness of thunderstorms being less prevalent within the catchments of the most flood-prone canyons. Unfortunately, two deaths resulted from an earlier flash flood (20 May 2023) in the Grand Staircase-Escalante National Monument with radar rainfall estimates of 2-4 cm near the slot canyon in which they became trapped (NCEI 2023).

This research relied upon the predominantly radar-based MRMS QPE analyses. While precipitation far from the KICX radar is likely underestimated, rainfall estimates from the MRMS across southwestern Utah appear reasonable. Estimates of rainfall and convection from station rain gauges, NLDN lightning, and MRMS QPE show the expected dependence on the underlying terrain with convection initiated at higher elevations during the afternoon. Also, as expected, widespread excessive summer rainfall in southwestern Utah generally occurs when the PWAT and CAPE are higher than typically observed across the region. The short time lag between early afternoon high CAPE and the onset of vigorous thunderstorms over the high terrain is often followed by subsequent downstream development that propagates above canyon headwaters by the prevailing flow.

The cumulative spatial and temporal variations of rainfall, moisture availability, and instability were examined during the three monsoon seasons. The prevailing conditions during 26 July 2021 were used to examine the factors contributing to seven flash floods, one in Cedar City, UT and the others scattered across several of the Parks in the region. PWAT and CAPE were unusually high relative to other days during the three summers with unidirectional flow from the southeast. The composite reflectivity above 60 dBz near Cedar City and other locales would put these storms near the 90th percentile of flash flood producing storms in the region (Smith et al. (2019).

During the three monsoon seasons, the HRRR generally provided accurate forecasts of the areal-averaged PWAT and under forecasted CAPE at all lead times out to 18 h, similar to other findings of HRRR forecasted CAPE and precipitation for convective events (Evans et al.

2018; Yue and Gebremichael 2020). The utility of using 12 member TLE means available 13-18 h prior to the typical onset of convection over the high terrain in the region was examined. Correcting for the negative CAPE forecast bias observed during the first two summers improved predictions of the conditions favorable for widespread rainfall during the 2023 summer. Using random forest classification with PWAT and CAPE as predictors for the upper quartile of areal-averaged rainfall showed promise at lead times relevant for operational predictions.

Repeating our analysis using TLE HRRR forecasts during summer 2024 will provide opportunities to test alternative machine learning strategies that might lead to improvements to the approach taken here. For example, each PWAT and CAPE forecast in the TLEs could be used as predictors, additional parameters could be considered (e.g., wind shear, HRRR QPE) or the domain could be confined to areas where flash floods are more likely or have higher impact (e.g., the areal extents of the Parks). The focus could also shift to predicting the extent within the domain of high rainfall rates (e.g., $\geq$ 1cm h^{-1}) rather than the daily rainfall total metric used here. Testing approaches for the entirety of southern Utah including areas with limited radar coverage would be possible by focusing on lightning as a proxy rather than MRMS QPE.

The operational transition of the HRRR to the Rapid Refresh Forecast System (RRFS) should be completed prior to summer 2025 (Dowell et al. 2022). Testing RRFS experimental output during summer 2024 may provide insight into how the approach developed here could take advantage of the six-member forecast ensembles to be available each hour as well as combining them over several initialization times into larger TLE ensembles. Loken et al. (2022) have explored random forecast approaches based upon individual ensemble members as well as averages over the ensemble sample. In addition, it will be possible to extend the lead time for which forecasts of this type are available out to 36 h. Grim et al. (2024) have compared HRRR and RRFS forecasts of organized convective systems during summer 2022 in the eastern U.S. There certainly will need to be similar studies undertaken to evaluate how well the RRFS handles the types of terrain-forced thunderstorms common to southwestern Utah and other regions within the western U.S.

Meyer and Jin (2016, 2017) and Zhang (2023) among many other studies have examined current and future trends of the NAM on the basis of downscaled global climate simulations. Since global and regional climate models have difficulty resolving precipitation over limited domains dominated by complex terrain such as southwestern Utah, downscaling proxy indicators of monsoonal strength (e.g., CAPE and PWAT as used in this study) may provide an approach to evaluate future changes in the NAM's northern extent.

Acknowledgements. We would like to thank W. J. Steenburgh, L. Dunn, R. Chase, and A. Jacques for their comments related to this research. We also wish to express our appreciation for staff members (Darren Van Cleave, David Church, and Glen Merrill) of the Salt Lake City National Weather Service Forecasts Office for their explanations of operational procedures used to forecast flash floods, feedback on this research, and access to data collected by their office. This work was possible thanks to the University of Utah Center for High Performance Computing (CHPC) for the computational hardware and the NOAA/National Weather Service Collaborative Science, Technology, and Applied Research (CSTAR) Program, Award NA20NWS4680046, through which this research has been supported. Creation of the HRRR-Zarr archive would not have been possible without an Amazon Sustainability Data Initiative Promotional Credits Award. We appreciate very much the work within our research group by T. Gowan, A. Jacques, and A. Kovac that made it possible to use and interpret the HRRR data. The first author acknowledges his role as a member of the Board of Directors of Synoptic Data PBC. Use of API services provided by Synoptic Data does not represent a conflict of interest.

Data Availability Statement. The HRRR-Zarr archive is publicly available in the AWS Open Data Registry, made possible by credits awarded from the Amazon Sustainability Data Initiative https://registry.opendata.aws/noaa-hrrr-pds/. Precipitation observations will be available from Synoptic Data PBC. MRMS QPE files are available from the Iowa State University archives. Processed data files of PWAT, CAPE and MRMS QPE used in the random forecast classification are available in the University of Utah Hive archive.

References

Adams, D. K., and A. C. Comrie, 1997: The North American monsoon. *Bull. Amer. Meteor. Soc.*, **78**, 2197–2213, https://doi.org/10.1175/1520- 0477(1997)078<2197:TNAM>2.0.CO;2

Adams, D. K., and E. P. Souza, 2009: CAPE and Convective Events in the Southwest during the North American Monsoon. *Mon. Wea. Rev.*, **137**, 83–98, https://doi.org/10.1175/2008MWR2502.1.

Benjman, S., S. S. Weygandt, J. M. Brown, M. Hu, C. R. Alexander, T. G. Smirnova, J. B. Olson, E. P. James, D. C. Dowell, G. A. Grell, H. Lin, S. E. Peckham, T. L. Smith, W. R. Moninger, J. S. Kenyon, and G. S. Manikin, 2016: A North American Hourly Assimilation and Model Forecast Cycle: The Rapid Refresh, 2016. *Mon. Wea. Rev.*, **144**, 1669–1694, https:/doi:10.1175/MWR-D-15-0242.1.

Blaylock, B. K., and J. D. Horel, 2020: Comparison of Lightning Forecasts from the High-Resolution Rapid Refresh Model to Geostationary Lightning Mapper Observations. *Wea. Forecasting*, **35**, 401–416, https://doi.org/10.1175/WAF-D-19-0141.1.

Boos, W. R., and S. Pascale, 2021: Mechanical forcing of the North American monsoon by orography. *Nature 2021 599:7886*, **599**, 611–615, https://doi.org/10.1038/s41586-021-03978-2.

Breiman, L., 2001: Random forests. *Machine learning*, **45**, 5-32. https://doi.org/10.1023/A:101093340432

Burke, P. C., Lamers, A., Carbin, G., Erickson, M. J., Klein, M., Chenard, M., ... & Wood, L. (2023). The Excessive Rainfall Outlook at the Weather Prediction Center: Operational Definition, Construction, and Real-Time Collaboration. *Bull. Amer. Meteor. Soc.*, **104**, E542-E562. https://doi.org/10.1175/BAMS-D-21-0281.1

Chase, R. J., Harrison, D. R., Burke, A., Lackmann, G. M., & McGovern, A., 2022: A machine learning tutorial for operational meteorology. Part I: Traditional machine learning. *Wea. Forecasting*, ***37***, 1509-1529.https://doi.org/10.1175/WAF-D-22-0070.1

Doswell, C. A., H. E. Brooks, and R. A. Maddox, 1996: Flash Flood Forecasting: An Ingredients-Based Methodology. *Wea. Forecasting*, **11**, 560–581. https://doi.org/10.1175/1520-0434(1996)011%3C0560:FFFAIB%3E2.0.CO;2

Dougherty, K. J., J. D. Horel, and J. E. Nachamkin, 2021: Forecast Skill for California Heavy Precipitation Periods from the High-Resolution Rapid Refresh Model and the Coupled Ocean–

Atmosphere Mesoscale Prediction System. *Wea. Forecasting*, **36**, 2275–2288, https://doi.org/10.1175/WAF-D-20-0182.1.

Douglas, M. W., R. A. Maddox, K. Howard, and S. Reyes, 1993: The Mexican Monsoon. *J Clim*, **6**, 1665–1677, https://doi.org/10.1175/1520 0442(1993)006<1665:TMM>2.0.CO;2.

Dowell, D. C., and Coauthors, 2022: The High-Resolution Rapid Refresh (HRRR): An Hourly Updating Convection-Allowing Forecast Model. Part I: Motivation and System Description. *Wea. Forecast*ing **37**, 1371–1395, https://doi.org/10.1175/WAF-D-21-0151.1.

Dunn, L. B., and J. D. Horel, 1994a: Prediction of Central Arizona Convection. Part I: Evaluation of the NGM and Eta Model Precipitation Forecasts. *Weather Forecast*, **9**, 495–507, https://doi.org/10.1175/1520-0434(1994)009<0495:POCACP>2.0.CO;2.

——, and ——, 1994b: Prediction of Central Arizona Convection. Part II: Further Examination of the Eta Model Forecasts. *Wea. Forecasting*, **9**, 508–521, https://doi.org/10.1175/1520-0434(1994)009<0508:POCACP>2.0.CO;2.

ElSaadani, M., W. F. Krajewski, and D. L. Zimmerman, 2018: River network based characterization of errors in remotely sensed rainfall products in hydrological applications. *Remote Sensing Letters*, **9**, 743–752, https://doi.org/10.1080/2150704X.2018.1475768.

Evans, C., S. J. Weiss, I. L. Jirak, A. R. Dean, and D. S. Nevius, 2018: An Evaluation of Paired Regional/Convection-Allowing Forecast Vertical Thermodynamic Profiles in Warm-Season, Thunderstorm-Supporting Environments. *Wea. Forecasting*, **33**, 1547–1566, https://doi.org/10.1175/WAF-D-18-0124.1.

Gowan, T. A., J. D. Horel, A. A. Jacques, and A. Kovac, 2022: Using Cloud Computing to Analyze Model Output Archived in Zarr Format. *J Atmos Ocean Technol*, **39**, 449–462, https://doi.org/10.1175/JTECH-D-21-0106.1.

Gourley, J. J., Erlingis, J. M., Hong, Y., & Wells, E. B., 2012: Evaluation of tools used for monitoring and forecasting flash floods in the United States. *Wea. Forecasting*, **27**, 158-173. https://doi.org/10.1175/WAF-D-10-05043.1 https://doi.org/10.1175/WAF-D-23-0112.1

Grim, J. A., Pinto, J. O., & Dowell, D. C., 2024: Assessing RRFS versus HRRR in Predicting Widespread Convective Systems over the Eastern CONUS. *Wea. Forecasting*,**39**, 121-140. https://doi.org/10.1175/WAF-D-23-0112.1

Gutzler, D. S., and Coauthors, 2009: Simulations of the 2004 North American Monsoon: NAMAP2. *J Clim*, **22**, 6716–6740, https://doi.org/10.1175/2009JCLI3138.1

Herman, G., and R. Schumacher, 2018: Flash flood verification: Pondering precipitation proxies." *J. Hydrometeor,* **19**, 1753-1776. https://doi.org/10.1175/JHM-D-18-0092.1

Hill, A. J., and R. Schumacher, 2021: Forecasting excessive rainfall with random forests and a deterministic convection-allowing model. *Wea. Forecasting*, **36**, 1693-1711. https://doi.org/10.1175/WAF-D-21-0026.1

Hu, M., S. G. Benjamin, T. T. Ladwig, D. C. Dowell, S. S. Weygandt, C. R. Alexander, and J. S. Whitaker, 2017: GSI Three-Dimensional Ensemble–Variational Hybrid Data Assimilation Using a Global Ensemble for the Regional Rapid Refresh Model. *Mon Weather Rev*, **145**, 4205–4225, https://doi.org/10.1175/MWR-D-16- 0418.1.

Iowa State University, 2023: Iowa Environmental Mesonet. https://mesonet.agron.iastate.edu/plotting/auto/ (Accessed 10 October, 2023

James, E. P., and S. G. Benjamin, 2017: Observation System Experiments with the Hourly Updating Rapid Refresh Model Using GSI Hybrid Ensemble–Variational Data Assimilation. *Mon. Wea, Rev*,. **145**, 2897–2918, https://doi.org/10.1175/MWR-D-16-0398.1.

Loken, E. D., Clark, A. J., & McGovern, A. (2022). Comparing and interpreting differently designed random forests for next-day severe weather hazard prediction. *Wea. Forecasting*, **37**, 871-899. https://doi.org/10.1175/WAF-D-21-0138.1

MacDonald, L. M., and C. J. Nowotarski, 2023: Verification of Rapid Refresh and High-Resolution Rapid Refresh Model Variables in Tornadic Tropical Cyclones. *Wea. Forecasting*, **38**, https://doi.org/10.1175/WAF-D-22-0117.1.

Maddox, R. A., Chappell, C. F., & Hoxit, L. R., 1979: Synoptic and mesoscale aspects of flash flood events. *Bull. Amer. Meteor. Soc*, **60**, 115–123. https://doi.org/10.1175/1520-0477-60.2.115

Maddox, R. A., D. M. McCollum, and K. W. Howard, 1995: Large-Scale Patterns Associated with Severe Summertime Thunderstorms over Central Arizona. *Wea. Forecasting*, **10**, 763–778, https://doi.org/10.1175/1520- 0434(1995)010<0763:LSPAWS>2.0.CO;2.

Marjerison, Rebecca D., et al., 2016: Does population affect the location of flash flood reports?. *J. Appl. Meteor. Climatol*., **55**, 1953-1963. https://doi.org/10.1175/JAMC-D-15-0329.1

Martinaitis, S. M., S. B. Cocks, M. J. Simpson, A. P. Osborne, S. S. Harkema, H. M. Grams, J. Zhang, and K. W. Howard, 2021: Advancements and Characteristics of Gauge Ingest and Quality Control within the Multi-Radar Multi-Sensor System. *J. Hydrometeorol.*, **22**, 2455–

2474, https://doi.org/10.1175/JHM-D-20-0234.1.

Martinaitis, S. M., Wilson, K. A., Yussouf, N., Gourley, J. J., Vergara, H., Meyer, T. C., ... & Monroe, J. (2023). A path toward short-term probabilistic flash flood prediction. *Bull. Amer. Meteor. Soc.*, **104**, E585-E605. https://doi.org/10.1175/BAMS-D-22-0026.1

McGovern, A., K. L. Elmore, D. J. Gagne, S. E. Haupt, C. D. Karstens, R. Lagerquist, T. Smith, and J. K. Williams, 2017: Using artificial intelligence to improve real-time decision-making for high-impact weather. *Bull. Amer. Meteor. Soc.*, **98**, 2073–2090, doi:10.1175/BAMS-D-16-0123.1.

Mazon, J. J., C. L. Castro, D. K. Adams, H.-I. Chang, C. M. Carrillo, and J. J. Brost, 2016: Objective Climatological Analysis of Extreme Weather Events in Arizona during the North American Monsoon, *J. Appl. Meteor. Climatol.*, **55**, 2431–2450, https://doi.org/10.1175/JAMC-D-16-0075.1.

Meyer, J. D. D., and J. Jin, 2016: Bias correction of the CCSM4 for improved regional climate modeling of the North American monsoon. *Clim Dyn*, **46**, 2961–2976, https://doi.org/10.1007/S00382-015-2744-5/METRICS.

——, and ——, 2017: The response of future projections of the North American monsoon when combining dynamical downscaling and bias correction of CCSM4 output. *Clim Dyn*, **49**, 433–447, https://doi.org/10.1007/S00382-016-3352- 8/METRICS.

Murphy, M. J., J. A. Cramer, and R. K. Said, 2021: Recent history of upgrades to the U.S. National Lightning Detection Network. *J Atmos Ocean Technol*, **38**, 573– 585, https://doi.org/10.1175/JTECH-D-19-0215.1.

NCEI, 2023: Storm Events Database. NOAA, accessed 5 December 2023, https://www.ncdc.noaa.gov/stormevents/.

Powell, J. T. (2023): *Analysis of Southwestern Utah Precipitation Events Associated With Flash Flooding.* University of Utah M.S. Thesis. 91 pp. (Order No. 30529315). Available from Dissertations & Theses @ University of Utah; ProQuest Dissertations & Theses Global.

Risanto, C. B., C. L. Castro, A. F. Arellano, J. M. Moker, and D. K. Adams, 2021: The Impact of Assimilating GPS Precipitable Water Vapor in Convective-Permitting WRF-ARW on North American Monsoon Precipitation Forecasts over Northwest Mexico. *Mon. Wea. Rev.*, **149**, 3013–3035, https://doi.org/10.1175/MWR-D-20- 0394.1.

Schumacher, R., 2017: Heavy rainfall and flash flooding. *Oxford research encyclopedia of natural hazard science*. 2017. https://doi.org/10.1093/acrefore/9780199389407.013.132

Schumacher, R. S., Hill, A. J., Klein, M., Nelson, J. A., Erickson, M. J., Trojniak, S. M., & Herman, G. R. (2021). From random forests to flood forecasts: A research to operations success story. *Bull. Amer. Meteor. Soc.,* 102(9), E1742-E1755. https://doi.org/10.1175/BAMS-D-20-0186.1

Serra, Y. L., and Coauthors, 2016: The North American Monsoon GPS Transect Experiment 2013. *Bull. Amer. Meteor. Soc.,* **97**, 2103–2115, https://doi.org/10.1175/BAMS-D-14-00250.1.

Sharif, R. B., E. H. Habib, and M. ElSaadani, 2020: Evaluation of Radar-Rainfall Products over Coastal Louisiana. *Remote Sens (Basel)*, **12**, https://doi.org/10.3390/rs12091477.

Smith, J. A., M. L. Baeck, L. Yang, J. Signell, E. Morin, and D. C. Goodrich, 2019: The Paroxysmal Precipitation of the Desert: Flash Floods in the Southwestern United States. *Water Resour Res*, **55**, 10218–10247, https://doi.org/https://doi.org/10.1029/2019WR025480.

Sun, J., and Coauthors, 2014: Use of NWP for Nowcasting Convective Precipitation: Recent Progress and Challenges. *Bull. Amer. Meteor. Soc.*, **95**, 409–426, https://doi.org/10.1175/BAMS-D-11-00263.1.

Thompson, G., M. K. Politovich, and R. M. Rasmussen, 2017: A numerical weather model's ability to predict characteristics of aircraft icing environments. *Wea. Forecasting*, **32**, 207–221, https:// doi.org/10.1175/WAF-D-16-0125.1.

Wilks, D. S., 2011: *Statistical Methods in the Atmospheric Sciences*. 3rd ed. International Geophysics Series, Vol. 100, Academic Press, 704 pp.

Xu, M., G. Thompson, D. R. Adriaansen, and S. D. Landolt, 2019: On the value of time-lag-ensemble averaging to improve numerical model predictions of aircraft icing conditions. *Wea. Forecasting*, **34**, 507–519, doi:10.1175/WAF-D-18-0087.1.

Yang, L., J. Smith, M. L. Baeck, and E. Morin, 2019: Flash Flooding in Arid/Semiarid Regions: Climatological Analyses of Flood-Producing Storms in Central Arizona during the North American Monsoon. *J Hydrometeorol*, **20**, 1449–1471, https://doi.org/10.1175/JHM-D-19-0016.1.

Yu, Guo, et al. "Seasonal Storm Characteristics Govern Urban Flash Floods: Insights from the Arid Las Vegas Wash Watershed." *J. Hydrometeorol.,* **24**, 2105-2123. https://doi.org/10.1175/JHM-D-23-0002.1

Yussouf, N.; Knopfmeier, K.H. Application of the Warn-on-Forecast system for flash-flood-producing heavy convective rainfall events. *Q. J. R. Meteorol. Soc.* **2019**, *145*, 2385–2403. https://doi.org/10.1002/qj.3568

Zhang, J., and Coauthors, 2016: Multi-Radar Multi-Sensor (MRMS) Quantitative Precipitation Estimation: Initial Operating Capabilities. *Bull. Amer. Meteor. Soc.*, **97**, 621–638, https://doi.org/10.1175/BAMS-D-14-00174.1.

Zhang, W., 2023: The dry and hot American Southwest under the present and future climates. *Atmospheric and Oceanic Science Letters*, 100340, https://doi.org/10.1016/J.AOSL